# Manifestation of attosecond XUV fields temporal structures in attosecond streaking spectrogram

**Guanglong Chen (陈光龙)[1], Yunjiu Cao (曹云玖)[1], and Dong Eon Kim[2*]**

[1] *School of Fundamental Studies, Shanghai University of Engineering Science, Shanghai 201620, China*

[2] *Department of Physics, Center for Attosecond and Technology (POTECH), Pohang 790-784, Korea*

[*] *Corresponding author: kimd@postech.ac.kr*

Received December 7, 2010; accepted January 6, 2011; posted online April 28, 2011

The features of an attosecond extreme ultraviolet (XUV) field are encoded in the attosecond XUV spectrogram. We investigate the effect of the temporal structures of attosecond XUV fields on the attosecond streaking spectrogram. Factors such as the number of attosecond XUV pulses and the temporal chirp of attosecond XUV pulses are considered. Results indicate that unlike the attosecond streaking spectrogram for an attosecond XUV field with two pulses of a half-cycle separation of streaking field, the spectrogram for the attosecond XUV field with three pulses demonstrates fine spectral fringes in separated traces.

*OCIS codes:* 320.7100, 300.6560, 270.6620.

*doi: 10.3788/COL201109.063201.*

Recent developments in few cycle laser technology have resulted in the successful generation of single isolated attosecond pulses in the extreme ultraviolet (XUV) region using high-order harmonic generation (HHG)[1,2]. The generation and application of a single isolated attosecond pulse have attracted significant attention as a very promising tool with unprecedented temporal resolution for studies of the electronic dynamics in atoms and molecules[3−9]. For the characterization of attosecond pulses, a technique called frequency-resolved optical gating for the complete reconstruction of attosecond bursts (FROG CRAB) was proposed[10,11] and later used successfully to characterize single isolated attosecond pulses[1,2]. In this method, the atoms are ionized using an attosecond XUV field in the presence of a near-infrared (NIR) laser field referred to as a streaking field. Thus, the resultant electron energy spectrum contains the time structure of the XUV and the NIR field. The electron energy spectra as a function of the delays are called the attosecond streaking spectrogram. By measuring the electron energy spectra at different delays between the NIR and the XUV field, the attosecond streaking spectrogram is obtained. The principal component generalized projections algorithm (PCGPA)[12] is typically used to retrieve and characterize the attosecond pulse from the attosecond streaking spectrogram.

Considering the complication of real attosecond XUV pulses in experiments, it is difficult to identify the features of attosecond pulses from the spectrogram at first sight. Several papers concerning this topic have investigated the effect of major features of an attosecond XUV field on the attosecond spectrogram[10,11,13−16]. To better understand the spectrogram and provide a more intuitive picture between the attosecond XUV field and the spectrogram, we theoretically investigate the attosecond streaking spectrogram for attosecond XUV field with a main pulse and one weaker satellite or two weaker satellites. Unlike the attosecond streaking spectrogram for an attosecond XUV field with two pulses of a half-cycle separation of streaking field, the spectrogram for the attosecond XUV fields of three pulses demonstrates fine spectral fringes in the separated traces. Note that simple attosecond pulses are used in our work to provide insight into the temporal structure of an attosecond field from the spectrogram. Helium atom is also used in our simulation.

In the attosecond streaking method, a photoelectron ionized by an attosecond XUV electric field experiences a periodic modulation in its energy by the NIR laser field. From the quantum mechanical point of view, the NIR field acts as an ultrafast phase modulator on the electron wavepacket produced by the attosecond XUV field. Under single active electron assumption and strong field approximation (SFA)[17], when an atom with ionization potential $I_p$ is ionized by an attosecond XUV electric field $E_{\rm X}(t)$ in the presence of a NIR laser field $E(t)$, the attosecond streaking spectrogram in atomic unit is given as[11]

$$S(\tau) = |a(\tau)|^2 = \left| -\mathrm{i}\int_{-\infty}^{+\infty} \mathrm{d}t \exp[\mathrm{i}\phi(t)] d_{\rm p}(t) E_{\rm X}(t-\tau) \exp[\mathrm{i}(W+\mathrm{I_p})t] \right|^2, \tag{1}$$

$$\text{where } \phi(t) = -\int_{t}^{+\infty} \mathrm{d}t' [p\cdot\mathbf{A}(t') + \mathbf{A}^2(t')/2], \tag{2}$$

$a(\tau)$ is the transition amplitude, $W = p^2/2$ is the electron energy of the final continuum state, $\mathbf{A}(t)$ is the vector potential of the NIR laser field [$E(t) = -\partial\mathbf{A}(t)/\partial t$], and $d_{p(t)}$ is the dipole transition element from ground state to continuum state with momentum $p(t)$, which is equal to the central momentum of the unstreaked electrons $p_0$ plus $\mathbf{A}(t)$. For a linearly polarized NIR laser field $E(t) = E_0(t)\cos(\omega t)$, $\phi(t)$ can be written as $\phi(t) = \phi_1(t) + \phi_2(t) + \phi_3(t)$[11], where

$$\phi_1(t) = -\int_{t}^{+\infty} \mathrm{d}t U_{\rm p}(t), \tag{3}$$

$$\phi_2(t) = \left[\sqrt{8WU_{\rm p}(t)}/\omega\right]\cos\theta\cos(\omega t), \tag{4}$$

 

$$\phi_3(t) = -[U_p(t)/2\omega]\sin(2\omega t). \quad (5)$$

Here, $U_p(t) = E_0(t)^2/(4\omega^2)$ is the ponderomotive potential of the electron and the angle between electron velocity and laser polarization direction $\theta$. In this letter, $\theta$ is set to be zero to maximize the streaking effect. An attosecond XUV field used in our calculation is assumed for simplicity as

$$E_X(t) = E_{X0}\exp(-2\ln 2t^2/t_0^2)\exp(i\omega_X t + ibt^2), \quad (6)$$

where $t_0$ is the pulse duration in the full-width at half-maximum (FWHM), $\omega_X$ is the central energy of the XUV pulse, and $b$ is the temporal chirp parameter.

A single isolated attosecond pulse was successfully produced through spectral filtering of the XUV radiation. However, it was difficult to completely suppress the energy contained in satellites generated at every half cycle of the NIR laser field. Thus, an attosecond field could consist of a main attosecond pulse and one or two weaker satellite pulses separated by half cycles of a streaking laser field[13,16]. We first conducted a simulation for an attosecond field consisting of a main pulse and one weak satellite pulse with a 4:1 peak intensity ratio ($E_X(t) + 0.5E_X(t - T/2)$, where $T$ is the cycle of the NIR laser field and is 2.7 fs for 800 nm), as shown in Fig. 1(a). In this work, unless otherwise mentioned, the delay time step was set to be about 39 as. The calculated attosecond streaking spectrogram is shown in Fig. 1(b). The attosecond pulse duration of 150 as and the central photon energy of 100 eV were used. The intensity and duration of the 800-nm NIR laser pulse were 7.5 TW/cm$^2$ and 5-fs FWHM, respectively. For comparison, the spectrograms for an isolated attosecond XUV pulse with $t_0$ of 150 as and $\omega_X$ of 100 eV are inserted in Fig. 1(b). Note that we made calculations to verify our calculated results and found that the results were in agreement with those in Ref. [11] under the same conditions.

From Fig. 1(b), the spectrogram is clearly different from that for a single isolated attosecond pulse from the following points: (1) spectral fringes are observed. The appearance of spectral fringes results from the interference between the two electron wave packets ionized by two attosecond pulses. The two attosecond pulses are separated by half a cycle of a NIR laser field; thus, the spectral fringe are spaced by 2 $\omega$~3.1 eV. (2) The spectral trace, particularly at the small delay time (corresponding to the high intensity of the streaking field) is separated into two parts: one is shifted to the higher energy and the other to the lower energy. On the one hand, the time separation between the two XUV pulses is half a cycle of the NIR laser field and the electron wave packet produced by one attosecond pulse is accelerated. On the other hand, the electron wave packet produced by the other attosecond pulse is decelerated by the streaking field. Obviously, when the spectral separation is not large, spectral interference fringes could be found between two separated spectral parts. Otherwise, there are no fringes between the two separated spectral parts. For example, at the delay time of about 3.3 fs in Fig. 1(b), the spectral could be observed clearly, while no fringes could be found at the delay time of about 0.7 fs. However, the intensities of the two separated spectral traces are different. The

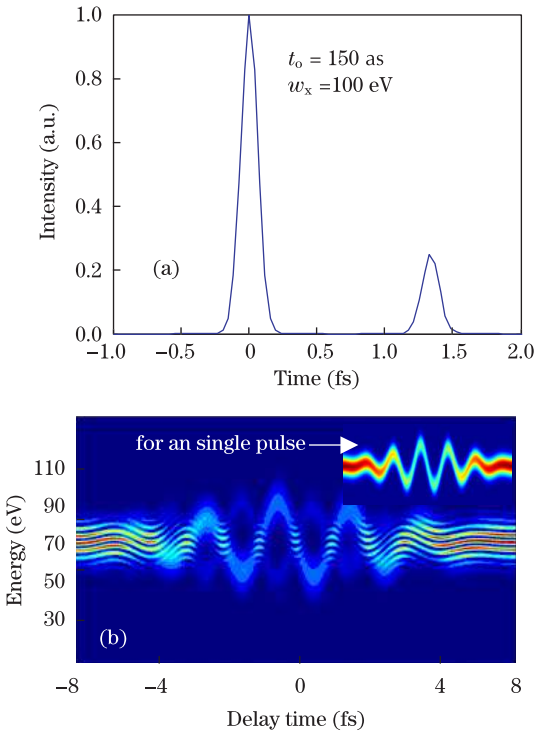


Fig. 1. (a) Attosecond XUV field with double pulses of a 4:1 peak intensity ratio, which are separated by a half-cycle of the IR laser field (1.33 fs). (b) The calculated attosecond streaking spectrogram of (a). The 800-nm 5-fs streaking NIR laser field with a peak intensity of 7.5 TW/cm$^2$ is used. The spectrogram for an isolated attosecond XUV pulse with $t_0$ of 150 as and $\omega_X$ of 100 eV is inserted in (b) for comparison.

spectrogram is determined mostly by the main pulse. Based on Eq. (1), the intensity of the spectrogram is related to the amplitude of XUV field $E_{X0}$. Hence, the large XUV field amplitude corresponds to the high intensity of the spectrogram (i.e., stronger trace). In our case, the main pulse shows the strong trace, while the weak satellite pulse shows the weak trace. Thus, the relative intensity of the accompanying satellite pulses in attosecond XUV field is indicated qualitatively by the intensity of the separated spectral trace, as discussed in Ref. [2].

To demonstrate the effect of the number of satellite pulses on the spectrogram further, an attosecond XUV field with a main pulse and two same satellite pulses is used to simulate the spectrogram, as shown in Fig. 2(b). The intensity ratio of the main pulse and satellite pulse is still set to be 4:1, but the attosecond XUV field is given by 0.5 $E_X(t+T/2)$ + $E_X(t)$ + 0.5 $E_X(t-T/2)$, as shown in Fig. 2(a). Similar to Fig. 1(b), the spectral fringes could be seen clearly due to the interference between the three electron wave packets ionized by the attosecond field. The spectral separation could also be found easily. However, different from that in Fig. 1(b), there are fine spectral fringes in either of the two separated spectral traces. The fine spectral fringes can be understood as the following. The weak separated trace results from the electron wave packets produced by the satellite pulse. The two satellites are separated by one cycle of streaking field $T$ and thus experiences the same phase gates by

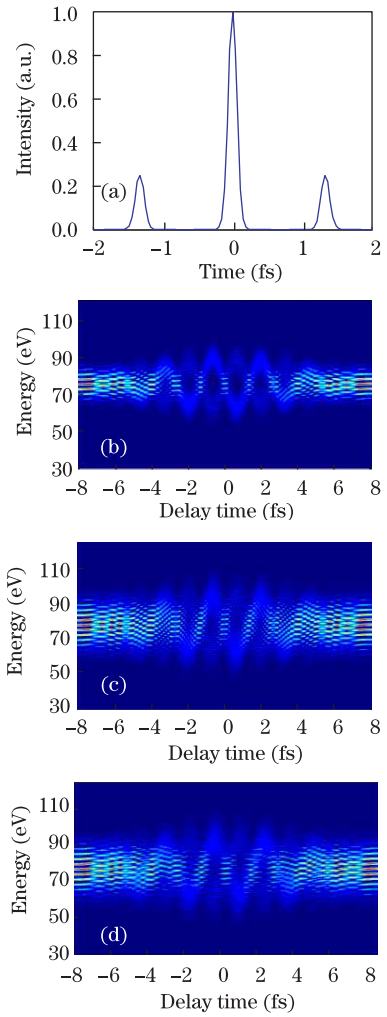


Fig. 2. (a) Attosecond XUV field consisting of one main pulse and two same satellite pulses of a 4:1 peak intensity ratio ($t_0 =$ 150 as). The calculated attosecond streaking spectrogram of (a) for a temporal chirp parameter, (b) $b = 0$ (the corresponding spectral bandwidth is 12.2 eV), (c) $b = 80$ fs$^{-2}$ (the corresponding spectral bandwidth is 19.9 eV), and (d) $b = 80$ fs$^{-2}$, while the delay time step is changed to about 233 as from 39 as. The other parameters are the same as in Fig. 1.

the streaking field and the energy spectra of electrons produced by the satellite pulse is in phase. The spectral traces from the two satellite pulses overlap and interfere, demonstrating fine spectral fringes. Thus, the fine spectral fringes encode the information of the satellite pulse number. We also investigate the effects of temporal chirp on the spectrogram using the three-pulse XUV field with a chirp. For simplification, the same chirp parameter $b$ (80 fs$^{-2}$) for the three pulses is assumed, as shown in Fig. 2(c), the wider spectral bandwidth can be found due to the temporal chirp. This is because a temporally chirped XUV pulse corresponds to a larger frequency bandwidth compared to that without a temporal chirp. For example, the FWHM of energy bandwidth at the delay time of 7 fs is about 12 eV in Fig. 2(b) and about 20 eV in Fig. 2(c). Note that the spectral fringes between the two separated traces can be found even at the delay time of about 0.7 fs in Fig. 2(c). These fringes result from the interference of spectral traces from the satellite pulses and the main pulse. In this case, the spectral fringes become more complex. For example, fringes between the two separated traces demonstrate a disconnection, as shown in Fig. 2(c). This results from the interferences of spectral traces from the three pulses, or the main pulse and two satellite pulses (Further detailed investigation concerning fringe disconnection is recommended). Despite the interference, fine spectral fringes can still be easily found. To further demonstrate the fine spectral fringes, we simulate the spectrogram using a large delay time step of 233 as, as shown in Fig. 2(d). Although the spectral fringes between the two separated traces show some changes, it is not difficult to find fine spectral fringes in the separated spectral traces. That is to say, in a real experimental situation, these fine spectral fringes could be important in identifying the number of satellite pulses, such as the temporal structure of an attosecond XUV field.

In conclusion, the manner by which the temporal structures of an attosecond XUV fields manifest in the attosecond streaking spectrogram has been investigated in detail to provide insight into the attosecond streaking spectrogram. For an attosecond field of multiple pulses, the spectral fringe and spectral separation can be observed in the streaking spectrogram. Spectral separation results from the time separation between two pulses by a half cycle of streaking field. The fine spectral fringes in the separated traces are related to the number of attosecond pulses with a time separation of a full cycle of a streaking laser field. The results of this work are necessary to understand further a streaking spectrogram and are helpful to quickly identify the main features of an attosecond pulse.

This work was supported in part by the BK21 project, the Basic Research Program (No. KRF-2008-313-C00356) funded by Korean Research Foundation and the Global Research Laboratory Program funded by National Research Foundation (No. 2009-00439).

## References

1. G. Sansone, E. Benedetti, F. Calegari, C. Vozzi, L. Avaldi, R. Flammini, L. Poletto, P. Villoresi, C. Altucci, R. Velotta, S. Stagira, S. De Silvestri, and M. Nisoli, Science **314,** 443 (2006).
2. E. Goulielmakis, M. Schultze, M. Hofstetter, V. S. Yakovlev, J. Gagnon, M. Uiberacker, A. L. Aquila, E. M. Gullikson, D. T. Attwood, R. Kienberger, F. Krausz, and U. Kleineberg, Science **320,** 1614 (2008).
3. R. Kienberger, E. Goulielmakis, M. Uiberacker, A. Baltuska, V. Yakovlev, F. Bammer, A. Scrinzi, Th. Westerwalbesloh, U. Kleineberg, U. Heinzmann, M. Drescher, and F. Krausz, Nature **427,** 817 (2004).
4. E. Goulielmakis, V. S. Yakovlev, A. L. Cavalieri, M. Uiberacker, V. Pervak, A. Apolonski, R. Kienberger, U. Kleineberg, and F. Krausz, Science **317,** 769 (2007).
5. M. Uiberacker, Th. Uphues, M. Schultze, A. J. Verhoef, V. Yakovlev, M. F. Kling, J. Rauschenberger, N. M. Kabachnik, H. Schröder, M. Lezius, K. L. Kompa, H.-G. Muller, M. J. J. Vrakking, S. Hendel, U. Kleineberg, U. Heinzmann, M. Drescher, and F. Krausz, Nature **446,** 627 (2007).
6. Y. Peng and H. Zeng, Phys. Rev. A **78,** 033821 (2008).
7. Y. Yu, J. Xu, Y. Fu, H. Xiong, H. Xu, J. Yao, B. Zeng, W. Chu, J. Chen, Y. Cheng, and Z. Xu, Phys. Rev. A

**80,** 053423 (2009).

8. X. Du, X. Zhou, and P. Li, Chinese J. Lasers (in Chinese) **37,** 1213 (2010).
9. V. S. Yakovlev, J. Gagnon, N. Karpowicz, and F. Krausz, Phys. Rev. Lett. **105,** 073001 (2010).
10. Y. Mairesse and F. Quéré, Phys. Rev A **71,** 011401 (2005).
11. F. Quéré, Y. Mairesse, and J. Itatani, J. Mod. Opt. **52,** 339 (2005).
12. D J. Kane, IEEE J. Quantum Electron. **35,** 421 (1999).
13. J. Gagnon, E. Goulielmakis, and V. Yakovlev, Appl. Phys. B **92,** 25 (2008).
14. H. Wang, M. Chini, S. D. Khan, S. Chen, S. Gilbertson, X. Feng, H. Mashiko, and Z. Chang, J. Phys. B: At. Mol. Opt. Phys. **42,** 134007 (2009).
15. J. Gagnon and V. Yakovlev, Opt. Express **17,** 17678 (2009).
16. M. Chini, H. Wang, S. D. Khan, S. Chen, and Z. Chang, Appl. Phys. Lett. **94,** 161112 (2009).
17. M. Lewenstein, Ph. Balcou, and M. Yu. Ivanov, Phys. Rev. A **49,** 2117 (1994).